Silicon (2023) 15:2113–2123
https://doi.org/10.1007/s12633-022-02138-z

ORIGINAL PAPER

Comparison of Rheological Methods to Obtain a Sufficient Sensitivity with Shear Interfacial Rheology in the Presence of Nanoparticles at Liquid/Liquid Interfaces

Thibault Roques-Carmes[1] · Maud Lebrun[1] · Yuqing Wang[1] · Diego Ramos[1] · Philippe Marchal[1] · Véronique Sadtler[1]

Received: 30 July 2022 / Accepted: 22 September 2022 / Published online: 13 October 2022

Abstract
Interfacial shear rheology can give a lot of information on the organization of the nanoparticles at the liquid/liquid and at the liquid/air interfaces. The measurements are challenging and not easy to conduct in a safe way to obtain reliable data. In the present study, the operating windows and the useful methods to obtain a reliable and sensitive response of the rheometer at the liquid/liquid interface in the presence of anchored nanoparticles are addressed. Hydrophobized silica adsorbed at the dodecane/water interface are mainly used while, in particular situations, non-ionic surfactant, and mixtures of nanoparticles and surfactant are also employed. The silica content is varied between 0.01 wt.% and 10 wt.% relative to the oil phase. Three mechanical solicitations modes and strengths of the interface including interfacial flow, creep, and oscillatory stress sweep at low amplitude are addressed in order to find the more sensitive and accurate one to probe the structural characteristics. The sensitivity and limits of the interfacial methods are significantly impacted by the strength and the mode of the mechanical solicitation applied to the dodecane/water interface. The oscillatory stress sweep at low amplitude appears as the most sensitive method since it allows to discriminate between the rheological behavior of the different silica contents and systems. It is recommended to use rheological methods for which the cumulated strain at the interface is moderate and does not destroy the structure of the silica film at the dodecane/water interface by the mechanical stress.

Keywords Interfacial rheology · Silica nanoparticles · Span surfactant · Dodecane/water interface, DWR · Particle laden fluid interfaces

1 Introduction

The majority of chemical formulated products involves nanomaterials [1–3]. Ice creams, sun screen lotions, toothpastes, lipsticks, paints, glues, bituminous binders are some examples. These chemical products are polyphasic systems where several phases (liquid, solid, gas) have to coexist leading to various interfaces. For all these systems, surfactants and polymers are currently used to stabilize the interfaces [4, 5]. The use of nanoparticles such as inorganic particles and bioparticles becomes an interesting alternative to the previous stabilizing molecules due to the high energy of desorption which protects the systems from destabilization by coalescence [6–11]. To reach the specific end-used properties required for these systems, a subtle combination of scientific disciplines comes into play [12, 13]. They include formulation science (dispersed systems, surfactants, nanoparticles), chemical engineering (mixing, emulsification processes), rheology (flowing, hydrodynamic and structural characteristic properties), and interfacial physico-chemistry (interfacial rheology, particles adsorption, surface tension, wetting). Among them, the behavior of the nanoparticles or nanomaterials at the various interfaces becomes a hot topic in this field [14–18].

Interfacial tension is traditionally the most widely studied characteristic of the interfacial phenomena. However, this method is not always sufficient to follow the structural and conformational transitions in the adsorption layers at the interfaces [19]. In addition, the surface and interfacial tension appears to be not substantially affected by the presence of particles at the interfaces. For all these reasons, interfacial

✉ Thibault Roques-Carmes
thibault.roques-carmes@univ-lorraine.fr

[1] Laboratoire Réactions Et Génie Des Procédés, Université de Lorraine, UMR 7274 CNRS, 1 rue Grandville, 54001 Nancy Cedex, France

rheology is expected to be more adapted to probe the adsorption, the structure and the conformation of nanoparticles at the liquid/gas or liquid/liquid interfaces [15, 16].

For interfacial rheology, the deformation of the interface can be produced by dilatation or shearing [15, 20]. On the one hand, for interfacial dilatational rheology, drop tensiometry and Langmuir film balance are currently encountered [20–25]. They are mainly used with surfactants and polymers. On the other hand, for interfacial shear rheology, the interface is directly sheared [26–29]. These latter systems have been recently developed and a clear view on the operating limits of these systems is still missing. For instance, the sensitivity with low molecular weight surfactants is not ensured. The rheometers appear more adapted to high molecular weight compounds such as polymers and particles [30].

One of the objectives of this work is to provide the operating windows and the useful methods to obtain a reliable and sensitive response of the rheometer at the liquid/liquid interface in the presence of anchored particles. Hydrophobized nanoparticles, non-ionic surfactant, and mixtures of particle–surfactant adsorbed at the dodecane/water interface are used. This silica can be viewed as a model system to ensure a relatively weak amount of silica at the interface while controlling the interfacial concentration of particles at the liquid/liquid interface. Various methods leading to different mechanical solicitations modes and strengths such as interfacial flow, creep, and oscillatory stress sweep at low amplitude are investigated. The aim is to find the more sensitive and accurate method to probe the structural characteristic properties of the interfaces. In parallel, a generic methodology is developed to help the readers to conduct interfacial rheology measurements and avoid classical errors.

2 Materials and Methods

2.1 Materials

The oily phase consisted of dodecane provided by ReagentPlus® with a purity larger than 99%. The nanomaterials were Aerosil® R-972 silica particles obtained from Evonik consisting of nanosized fumed silica particles with a diameter of 16 nm. The particles were hydrophobized by the grafting of dimethyl chlorosilane in order to obtain a coverage of 70% of the silanol groups of the silica. Span 65 is a sorbitan tristearate and was provided from Aldrich. It is a non-ionic lipophilic surfactant (HLB = 2.1).

For all the measurements, the particles and/or surfactants were introduced in dodecane. The silica was dispersed in the oil using an ultrasounds probe (Sonic Dismembrator 550 from Fisher Scientific-20 kHz frequency-standard probe). The sonication was performed during 1 min 30 s in sequence of 2 s of sonication followed by 2 s without sonication. The amplitude of sonication was fixed to 70% of its maximum amplitude. An ice bath was placed under the beaker to reduce the increase of temperature during the sonication. The hydrophobic character of the silica produced an instantaneous dispersion of the particles in the oil. The sonication was only used to finalize the homogenization of the dispersion. The hydrophobic character of the silica lead to a repartition of the silica between the oil phase and the interface. The particles had an amphiphilic behavior and they adsorb at the liquid/liquid interface. However, due to the hydrophobic character of the solid material, a high amount of silica was necessary to obtain a significant content of particles at the liquid/liquid interface. Consequently, for low silica content introduced in the oil, the interfacial concentration of silica at the liquid/liquid interface was very low. This adsorbed amount of silica increased with the silica fraction introduced in the oil. The silica content was varied between 0.01 wt.% and 10 wt.% relative to the oil phase. For silica content lower than or equal to 1 wt.%, the silica interfacial layer may not be fully covered, or may have large voids, which impacted rheological signature.

For the preparation of the surfactant solution, the Span 65 was dissolved in dodecane under magnetic agitation at a concentration of 0.5 mM. Deionized water was utilized for the aqueous phase.

2.2 Methods for Interfacial Shear Rheology Experiments

An AR-G2 stress-controlled rheometer from TA Instrument was used to conduct the interfacial shear rheology experiments. The rheometer was equipped with a diamond-edged ring made of Pt/Ir and a holding trough made of Teflon that is equivalent to a double wall ring (DWR) geometry. Figure 1 shows a schematic representation of the overall system. Prior to measurements, the ring was thoroughly cleaned. First, the ring was flame treated. Then, the ring was rinsed with water, ethanol, and finally dried. In parallel, the holding trough made of Teflon was cleaned with water and ethanol, and finally dried.

The most delicate point of experiences with DWR was to accurately and precisely locate the ring at the interface of the two liquids (Fig. 1). A special procedure was developed. In a first step, the water phase was introduced inside the holding trough made of Teflon up to the middle edge of the reservoir. At that moment, the diamond-edged ring was moved down until the moment it started to touch the water surface. In the vicinity of the water surface, the speed of the head was lowered to improve the precision. From that position, a diminution of 500 µm was applied to accurately positioned the ring at the liquid/liquid interface. Actually, 500 µm corresponded to one-half of the height of the ring. The addition of the oily phase

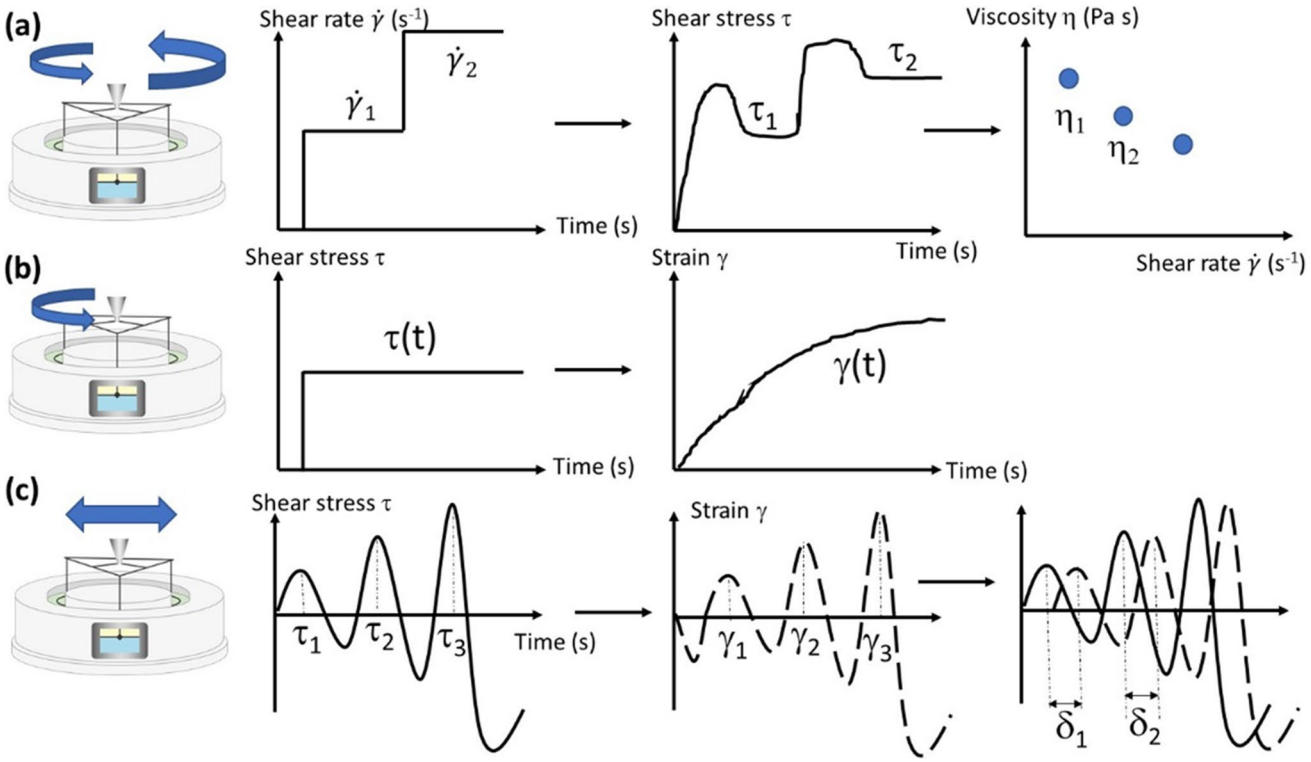

Fig. 1 Schematic representation of the interfacial rheological methods. (**a**) Steady-state flow tests, (**b**) Creep experiment, and (**c**) Oscillatory stress sweep at low amplitude. Colors: blue corresponds to the aqueous phase while yellow represents the oil phase

on the surface of the ring and the water was then made with a dropper. Care was taken to deposit the oil everywhere over the surface of water and the ring. A volume of 5 mL of the oily phase was added. The temperature was maintained at 25 °C for all the tests thanks to a Peltier plate.

Several interfacial rheological methods were conducted with the rheometer. All the methods used were based on the shearing of the liquid/liquid interface due to the rotation of the ring. The methods differed by the mechanical solicitation modes and strengths (Fig. 1).

The first method was to perform steady-state flow tests (Fig. 1a). In that case, the ring turned continuously and the speed of rotation was varied from low speed (low shear rate $\dot{\gamma}$) to high speed (high shear rate $\dot{\gamma}$). More particularly, successive steps of shear rate were imposed during a given time ($\dot{\gamma}_n$: $\dot{\gamma}_1$, $\dot{\gamma}_2$…) and the average value of the resulting shear stress (τ_n: τ_1, τ_2…) was recorded when the steady state was reached. The viscosity η was obtained from the ratio of the shear stress to the shear rate, i.e.:

$$\eta_n = \frac{\tau_n}{\dot{\gamma}_n} \tag{1}$$

In practice, steady state tests were performed by shearing the interface with shear rate starting at 10^{-4} s^{-1} up to 10 s^{-1}. From this test, the interface viscosity was recorded.

For the second method, creep tests experiments were carried out. For this test, a constant step of shear stress was applied and the resulting strain of the interface was followed with time (Fig. 1b). In that case, the shear stress was imposed and the measurement was conducted in transient regime. Experimentally, a constant shear stress of 10^{-5} N/m was imposed onto the interface. The creep analysis allowed to probe the response of the interface during very long time.

The third method concerned oscillatory mode. Oscillatory stress sweep experiments at low amplitude consisted in applying small amplitude oscillatory stress to the interface. The oscillatory shear stress and the angular frequency were imposed (Fig. 1c). In details, amplitude sweeps were conducted. The sinusoidal shear stress was increased stepwise from one point to the next while keeping the frequency at a constant value. The resulting evolution of the shear strain was recorded leading to a sinusoidal evolution of the strain. The comparison of the two sinusoidal curves was conducted. From the phase shift angle (δ_n : δ_1, δ_2, δ_3…) and the maximum shear stress (τ_n: τ_1, τ_2, τ_3) and strain (γ_n: γ_1, γ_2, γ_3…), the interfacial elastic G' and viscous G'' modulus were deduced. They corresponded to a viscoelastic behavior of the interface with two extremes situations. For G'' = 0, a purely elastic interface was obtained while, when G' = 0, a purely viscous interface took place. The determination of G' and G'' could be obtained from:

$$\tau_{n^{(*)}} = \tau_n e^{i\omega t} \tag{2}$$

$$\gamma_{n^{(*)}} = \gamma_n e^{i(\omega t - \delta)} \tag{3}$$

$$G^* = \frac{\tau_{n^{(*)}}}{\gamma_{n^{(*)}}} = \frac{\tau_n}{\gamma_n} e^{i\delta} = \mathrm{G}' + \mathrm{iG}'' \tag{4}$$

where G* is the complex viscoelastic modulus. In addition, the relation between the phase shift angle and the viscous and elastic modulus was given by:

$$\tan\delta = \frac{G''}{G'} \tag{5}$$

$$G' = |G^*|\cos\delta \tag{6}$$

$$G'' = |G^*|\sin\delta \tag{7}$$

In our experiments, the oscillatory stress was applied between 10^{-6} and 10^{-1} N/m, and the angular frequency was fixed to 1 rad/s. With this test, the applied stress remained weak and allowed to preserve the structure of the silica film at the water/dodecane interface in the linear viscoelastic domain of the sample. Actually, the stress gently deformed the interface in the linear viscoelastic domain of the sample for which the strain remains proportional to the stress.

2.3 Equipment Performance Tests with Surfactant

The most important point when conducting experiments with DWR is to place the ring just at the interface between water and dodecane. Before testing with silica, several experiments were carried out with water/air systems in order to find ways to put the ring at the interface and get the accurate position of the ring at the interface (not shown). To ensure that the equipment perform normal, the performance of the apparatus is tested by measuring the interfacial shear properties (strain sweep and frequency sweep) of Span 65 at the water/dodecane interface. The results can be compared with the data reported in the literature. Actually, researchers from the company TA instruments have used the DWR with the same system, i.e. water/dodecane in the presence of Span 65 [31]. A concentration of 0.5 mM of surfactant in the dodecane phase was employed for measuring while for the water distilled water was used [31]. The evolution of the interfacial elastic and viscous modulus as a function of the strain and frequency are given in Fig. 2 and Fig. S1 of the Supplementary Information, respectively.

The results of the tests conducted here correspond well with those reported by the company TA Instruments which are used as a kind of calibration test of the apparatus [31]. The surfactant builds a viscoelastic film at the interface between water and dodecane. Consequently, it can be concluded that we find the way to accurately place the ring at the interface. Therefore, the equipment can be safely used with the other systems (water/dodecane in the presence of silica).

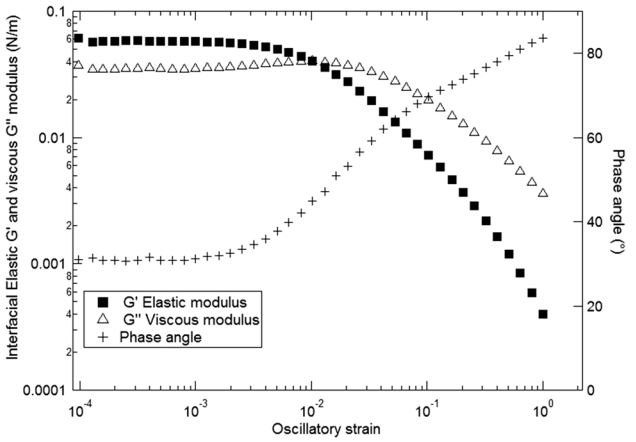

Fig. 2 Strain sweep experiment for Span 65 film at the interface between water and dodecane. The angular frequency was fixed to 1 rad/s

3 Results and Discussion

3.1 Evaluation of the Sensitivity of the Methods with Different Nanoparticles Contents

3.1.1 Time to Reach the Stationary Regime

When conducting shear interfacial rheology, it appears that the rheological data including interfacial viscosity, interfacial elastic and viscous modulus depend on the time after which the phases (aqueous and oil) are put into contact. This is not surprising since all the particles are initially located inside the oil phase. To modify the evolution of the rheological properties as compared to that of pure clean water/dodecane interface some particles need to be anchored at the interface. It is then important to measure a reliable rheological signal which corresponds really to a situation where the maximum amount of particles is adsorbed at the interface. This situation might correspond to the stationary state. In order to determine the characteristic time needed to reach this stationary state, oscillatory experiments were performed at different times after the contact between the two phases. The results are reported in Fig. 3 and correspond to a silica content of 0.1 wt.% in dodecane.

Just after the contact between the two phases (t = 0 h), the evolution of G' with the oscillatory stress is similar to that observed for the bare clean water/dodecane interface. This result is not surprising since the particles had no time enough to diffuse and adsorb at the dodecane/water interface.

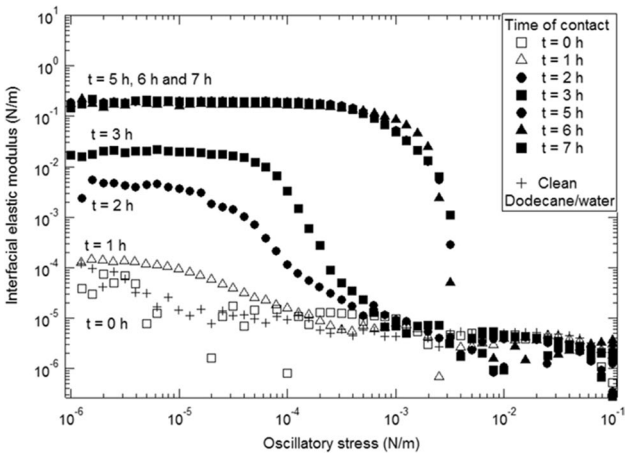

Fig. 3 Influence of the time after the contact between the two phases on the evolution of the interfacial elastic modulus *vs* the oscillatory stress. Silica content of 0.1 wt.% in dodecane. The angular frequency was fixed to 1 rad/s

During the five first hours, the interfacial elastic modulus G' *vs* oscillatory stress increases with the time. The increase of G' with the time attests of the progressive adsorption of the silica particles with time. The measurements conducted after 5 h, i.e. 6 h and 7 h, lead to similar evolutions than that reported at 5 h. Consequently, the time needed to reach constant value of G' is equal to 5 h. In other words, 5 h are necessary to reach the steady state. In addition, the experiments show a linear increase of G' at the plateau in the linear viscoelastic region (G' Plateau) with the time in a log–log scale in the range of times explored from 1 to 5 h (Fig. S2 of the Supplementary Information).

To confirm the above results, similar types of experiments were carried out with a silica content of 1 wt.% initially located in the dodecane. The results are depicted in Fig. S3 of the Supplementary Information. The same trend as above is observed. At t = 0 h, the curve coincides with that of pure dodecane/water interface. Then, the G' *vs* oscillatory stress curves increase with the time of contact between the two phases during the first 3 h (t = 1, 2 and 3 h). Oscillatory sweep experiments conducted at longer times produce no significant difference in the G' *vs* oscillatory stress signals. This indicates that 3 h is sufficient to monitor a signal corresponding to a stationary regime.

In the following, the same approach was employed for all the samples and only the curves for which G' becomes independent of the time were used. In addition, the influence of the silica content on the time to reach the stationary regime is reported in Table 1. It appears that the time needed to reach the maximum modulus, i.e. the steady state, depends on the silica amount. The time decreases as the silica concentration is enhanced. It can be also noticed that a power law evolution is recorded (Fig. S4 of the Supplementary Information). As an example, 1 h is necessary for 10 wt.% of silica while we have to wait 26 h when 0.01 wt.% of silica is utilized. This phenomenon may be interpreted since the higher concentration sample contains more particles and then some particles are already close to the interface of water and oil. Consequently, they can reach it faster because the distance to go to the interface is lower. This behavior is in accordance with results reported in literature [32]. Consequently, these times (Table 1) have been selected for the initial period prior to the rheological measurements in the following. For instance, the measurements with 1 wt.% of silica were conducted after 3 h of equilibration while 5 h were necessary when the particle content is equal to 0.1 wt.%.

Table 1 Influence of the silica concentration on the time needed to reach the stationary regime

Concentration of silica in dodecane (wt.%)	Time to reach stationary regime (h)
0.01	26
0.1	5
1	3
10	1

3.1.2 Flow Curves

Figure 4 displays the evolution of the viscosity of the dodecane/water interface as a function of the shear rate for various silica concentrations of 0, 0.1, 1 and 10 wt.%.

For all samples, the viscosity decreases with the shear rate. On the one hand, the flow curves for the silica contents of 0 (absence of silica), 0.1, and 1 wt.% are similar and collapse to a single one. The Newtonian plateau is obtained for shear rates lower than 10^{-3} s^{-1}. For larger shear rates, the viscosity decreases with the shear rate. On the other hand, the viscosity of the interface is significantly larger in the presence of 10 wt.% of silica. A very large amount of silica appears necessary to observe a difference between the rheological behaviors. Moreover, when the shear stress is plotted with respect to the shear rate, pertinent information can be also obtained (Fig. 5). For silica concentration of 10 wt.%, the shear stress remains constant regardless of the shear rates. This can be attributed to a lubricated friction of the ring on the edge of the silica film. In other words, when the ring spins faster, the particles anchored at the water/dodecane interface do not move leading to a frictional regime for which the stress remains constant according to the Coulomb's frictional law and the flow is not homogeneous. For the other silica concentrations, the shear stress increases with the shear rate up to a shear rate of 0.1 s^{-1}. For larger shear rates, the shear stress does

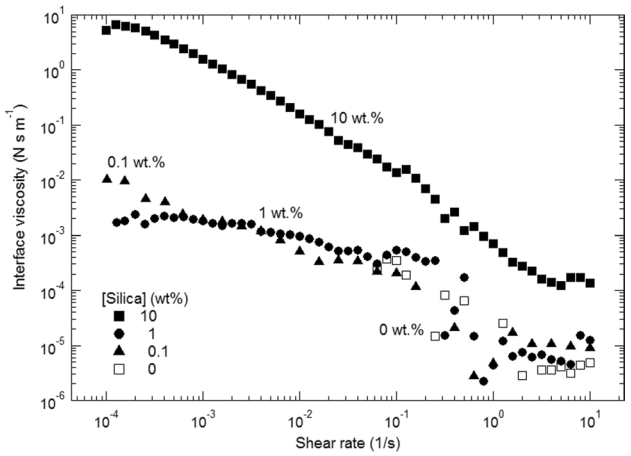

Fig. 4 Flow curves of dodecane/water interface in the presence of different concentrations of silica. Interface viscosity as a function of the shear rate

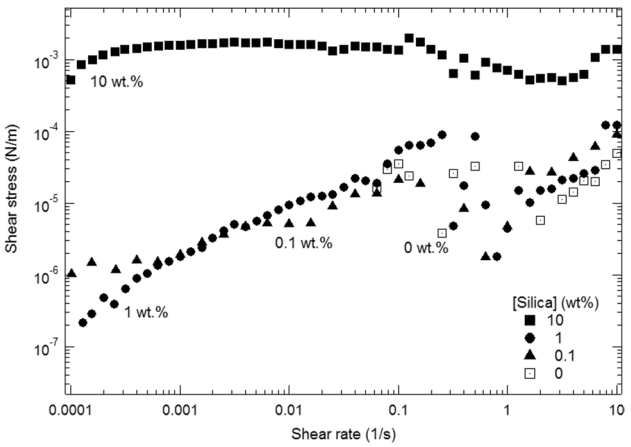

Fig. 5 Flow curves of dodecane/water interface in the presence of different concentrations of silica. Shear stress as a function of the shear rate

not vary. This highlights that shear rates larger than 0.1 s^{-1} are too large since they produce a lubricated friction of the ring on the silica film at the interface leading to a frictional regime characterized by a constant shear stress. In addition, at these high shear rates, the shear field might no longer be properly defined.

This first set of experiments reveals that a very large amount of silica is necessary to observe a difference between the flow curves. This highlights that the method is not sufficiently sensitive to discriminate between the interfacial rheological behavior of the interfaces with 0, 0.1 and 1 wt.% of silica. To our knowledge, no systematic study that makes this point was already reported in the literature.

3.1.3 Creep Curves

In a second step, creep experiments of water/dodecane interfaces with various concentrations of silica (0, 0.01, 0.1, 1 and 10 wt.%) were carried out. For these experiments, a constant stress of 10^{-5} N/m was applied and the strain at the interface was followed with time. The creep analysis allows to probe the response of the interface during very long time, the applied stress remaining inside the linear viscoelastic domain of the sample. The results are depicted in Fig. 6.

All the curves show the same evolution coherent with a viscoelastic behavior of the interfaces. Three zones can be extracted from the curve (Fig. S5 of the Supplementary Information). At short time, the strain increases steeply with time. This zone corresponds to the instantaneous elasticity of the sample. Then, a lower increase of the strain with time is recorded. This area is related to the retarded elasticity. At long time, the last zone called creep zone characterizes the viscous flow behavior of the interface. In summary, all the samples show a dominant viscous behavior of the interface at long time and an elastic behavior at short time. In the following, we discuss more precisely the final height of the creep zone. The height of the creep zone is inversely proportional to the rigidity of the interface. The presence of particles leads to a rigidification of the interface since the largest height of the creep zone is obtained in absence of particle with the bare dodecane/water interface. More precisely, the data can be divided into three categories depending on the silica concentration. A very low strain is reached for 10 wt.% silica. According to the duration of the experiment (250 s), the maximum strain value in the creep zone is around 10^{-4}. The curve at 10 wt.% of silica with a very weak value of

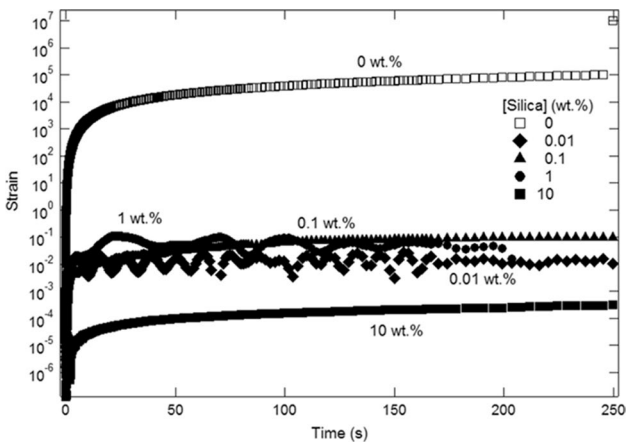

Fig. 6 Creep of the adsorption layer of silica at the dodecane/water interface with different concentrations of silica. A constant stress of 10^{-5} N/m was applied

the strain attests that the silica structure at the liquid/liquid interface produces the largest rigidification of the interface. On the opposite, in absence of silica, the value of the strain becomes significantly larger, i.e. 10^5. The curves for the other silica concentrations are situated in between these 2 extremes. However, no difference between the curves occurs regardless of the silica concentration for the interfaces with intermediate silica amounts. The difference between the curves and that at 0 wt.% is high while a lower deviation takes place with the creep curve at 10 wt.%. In addition, the strain values around 10^{-1}—10^{-2} in the creep zone indicate that the interfaces are a little stiff for the silica concentrations between 0.01 and 1 wt.%.

In conclusion, the creep method is more sensitive than the flow curves. However, the creep method is still not well suited to probe a difference between the liquid/liquid interfaces with 0.01, 0.1 and 1 wt.% of silica.

3.1.4 Oscillatory Stress Sweep at Low Amplitude

The last method concerns the oscillatory mode at low amplitude. The range of the applied stress is similar than those previously applied during the creep analysis and the flow experiments. The evolution of the elastic and viscous interfacial modulus as a function of the oscillatory stress for various silica concentrations is reported in Fig. 7 and Fig. S6 of the Supplementary Information, respectively.

The interesting feature is that all the curves are different for each silica concentration. In other words, the viscoelastic moduli, both G' and G'', increase with the silica content. These results point out that the oscillatory mode at low amplitude is more sensitive to probe the effect of the silica content at the interface. It is due to the fact that the structure of the silica at the dodecane/water interface is not broken by the mechanical stress in the linear zone. On the contrary, it can be observed that all the curves converge in the non-linear domain beyond stresses of 10^{-2} N/m. The two extremums borders, 0 wt.% and 10 wt.% silica, are still present as borders. The low interfacial elastic modulus G' in absence of silica attests of a liquid interface. On the opposite, at 10 wt.% of silica, the interface becomes rigid with an interfacial elastic modulus of 1.75 N/m. The interfacial G' for the other silica concentrations fall between these two values. In addition, the G' values increase with the silica content. It is interesting to note the regular evolution of the G' at the plateau in the linear viscoelastic region (G' Plateau) with the silica concentration. More particularly, a linear evolution in a log–log scale is obtained (Fig. S7 of the Supplementary Information). The shift of the amount of silica from 0 (absence of silica) to 0.01 wt.% produces a significant enhancement of the interfacial elastic modulus from 10^{-4}—10^{-5} N/m to 4 10^{-2} N/m. In the presence of silica, the interface becomes viscoelastic. The non-neglectable value of G' emphasizes that the particles touch each other. As a consequence, a contact particles-particles network takes place at the interface. When increasing the silica content, the rise of the interfacial elastic modulus confirms the enhancement of the solid character of the interface due to the silica network at the interface. The value of the interfacial elastic modulus depends on the number of links between the particles and the intensity of these links. The modulus increases when the number of links between the particles is enhanced and also if the link between the particles is harder [32].

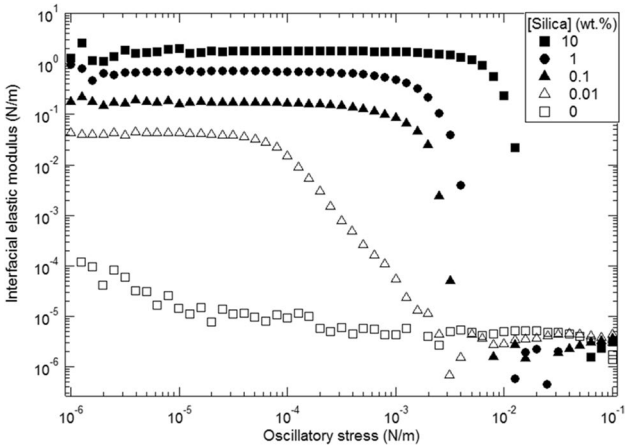

Fig. 7 Oscillatory stress sweeps. Interfacial elastic modulus *vs* the oscillatory stress in the presence of different concentrations of silica. The frequency was fixed to 1 rad/s

Another way to analyze the data is to report the interfacial elastic modulus data as a function of the strain (γ). The results are displayed in Fig. S8 of the Supplementary Information. The linear viscoelastic regime for which the interfacial elastic modulus does not vary with the strain is recorded at low shear strain. For larger strain, a diminution of the interfacial elastic modulus with the strain occurs. This zone corresponds to the breaking of the particles network at the interface. The cross-over strain between the two regions corresponds to the onset of strain for which the network of particles begins to be destroyed. It is written as γ_c in the following and can be used to probe the extent of the interaction between the particles at the interface. It appears here that the linearity domain, i.e. the linear viscoelastic regime, does not depend on the silica content. In other words, γ_c is around 10^{-3} regardless of the amount of silica. This indicates that the extent of the interaction between the particles at the interface is not impacted by the silica content. This result is not really surprising as only a change of oil, pH, ionic strength, surfactant or addition of other additives impact the interaction strength between the particles at the interface [15, 16].

3.1.5 Discussion of the Difference of Sensitivity Between the 3 Rheological Methods

Prior to discuss the difference of sensitivity between the 3 rheological methods, it appears necessary to discuss the structure of the interfacial layer of silica. Due to the hydrophobic character of the solid material a high amount of silica is necessary to obtain a significant content of particles at the liquid/liquid interface. Consequently, for low silica content introduced in the oil, the interfacial concentration of silica at the liquid/liquid interface is very low. For silica content lower than or equal to 1 wt.%, the silica interfacial layer may not be fully covered, or may have large voids, which impact rheological signature. The weak amount of silica at the interface is relevant to discriminate between the sensitivity of the different rheological interfacial methods.

The 3 rheological methods apply similar ranges of shear stresses. For the steady tests flow (η vs $\dot{\gamma}$), the apply shear stress is between 10^{-7} and 10^{-3} N/m. For the creep analysis (γ vs t), the shear stress is 10^{-5} N/m. In the oscillatory mode (G' vs τ), the shear stresses are between 10^{-6} and 10^{-2} N/m. However, the difference in sensitivity can be attributed to both (i) the direction of rotation of the ring and (ii) the cumulated strain applied to the interface. For the flow curves and creep analysis, the permanent unidirectional rotation of the ring produces a friction of the ring on the silica film. This configuration leads to a relatively weak sensitivity which is not sufficient to distinguish between the interfaces with various silica contents. Conversely, for the oscillatory stress sweep, the ring does not turn in a constant direction but oscillates around an equilibrium position. This setting does not generate lubricated friction of the ring on the particles at the interface. Consequently, this oscillatory mode appears as the most sensitive method since it allows to discriminate between the rheological response of the different interfaces bearing different silica contents.

Another way to discuss the sensitivity of the methods consists in analyzing the cumulated strain applied to the interface by each method. The cumulated strain or total strain applied to the interface depends on the strength of the rate of deformation ($\dot{\gamma}$) and on the time during which the deformation is applied. In other words, the cumulated strain, denoted as cumulated γ reads as:

$$\text{Cumulated } \gamma = \int \dot{\gamma} dt \tag{8}$$

For the flow curve (Fig. 1a and Fig. 5), the cumulated strain can be obtained by summing each product of the shear rate with the time for which this shear is applied. This summation is performed from low shear rates to high shear rates. As a consequence, the cumulated strain becomes very large. In addition, this high cumulated strain explains also the weaker quality of the data recorded for shear rates above 0.1. For the creep analysis (Fig. 1b and Fig. 6), the cumulated strain is enhanced also with the time during the experiments. On the opposite, the cumulated strain is significantly reduced during the oscillatory stress sweep since the oscillatory mode imposed to the ring maintains the maximum strain below 10^{-3} in the linear viscoelastic regime (Fig. 1c and Fig. S8 of the Supplementary Information).

The conclusions presented in the paper concern hard particles but the question arises also with soft particles or macromolecules such as proteins. Concerning the interfacial flow measurements, the ring friction problems (lubricated friction) are still present with soft particles or polymers [33–35]. However, the problem of friction of the ring is less critical with macromolecules such as proteins which seems to show that there could be a relatively continuous evolution when we go from hard particles to polymers through soft particles [33–36]. However, the lubricated friction of the ring problem remains in all three cases at varying levels. The creep tests show the same tendency regardless of the type of particles, i.e. hard, soft and proteins [34, 37]. In other words, the creep data have a better sensitivity than flow but a lower sensitivity than oscillatory tests [34]. The general trend shows that all improves when the particles go from rigid (hard particles) to molecular (macromolecules or proteins). However, with the 3 materials (hard, soft particles and proteins), the order of sensitivity is similar with oscillatory tests more accurate than creep and flow experiments. For all the systems, the oscillatory mode leads to more reliable measurements [16, 33–36].

3.2 Mixture of Surfactant and Particle

Finally, to confirm the high sensitivity of the method based on oscillatory stress amplitude sweep, the results obtained with Span 65 and silica are compared with those recorded with mixture of surfactant and particle. It is expected that the elasticity of the interface is improved in the presence of a mixture of particles and surfactants [38–40]. Here, the silica content is equal to 0.1 wt.% and the amount of Span 65 is 0.5 mM. The results of the mixture are compared to those obtained in the presence of silica alone (0.1 wt.%) and Span 65 alone (0.5 mM). The results are depicted in Fig. 8.

In the presence of the mixture of Span 65 and silica particle, a large elastic modulus is recorded. More interestingly, the highest elastic modulus occurs with the mixture. This indicates that a composite of surfactant and particle is created at the interface. This kind of result was already reported [38–40]. The lowest elasticity curve is reached with the surfactant alone. The elasticity with only silica goes in between the surfactant and the mixture of silica and Span 65. This confirms that the sensibility of the method based on oscillatory stress amplitude sweeps is sufficiently high to observe substantial difference between the 3 configurations at the interface. The order of the curves is

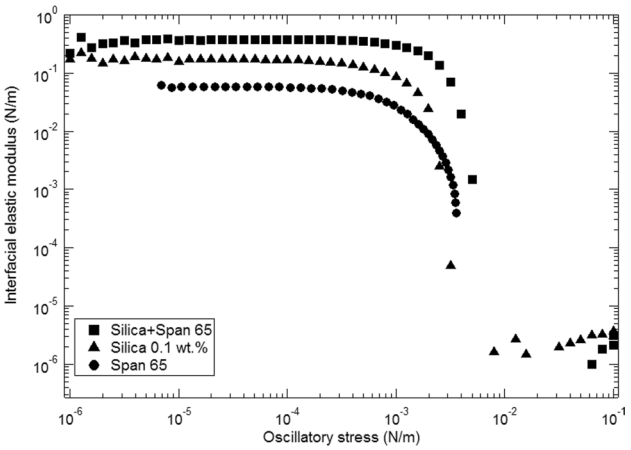

Fig. 8 Oscillatory stress sweeps. Interfacial elastic modulus vs the oscillatory stress in the presence of silica, Span 65 and mixture of Span 65 and silica. The frequency was fixed to 1 rad/s

consistent with the expected elasticity at the interface. In other words, the elasticity of particle is larger than that of surfactant alone. In addition, the mixture of the two components improves the elasticity of the interface. In the present study, the oscillatory stress amplitude sweeps method was the only one sufficiently sensitive to discriminate between the 3 samples.

Moreover, when the data are plotted as a function of the strain (Fig. S9 of the Supplementary Information) additional information can be obtained. When comparing the data with pure particles and surfactant alone, an extension of the linear viscoelastic regime is observed in the presence of surfactant. Actually, γ_c shifts from 10^{-3} to 10^{-2} when the silica particles are replaced by the Span 65. This increase was anticipated since the mobility of the surfactant molecules at the interface is larger than that of the particles [15, 16]. For the mixture of surfactant and particle, the linear viscoelastic regime and γ_c are similar to those obtained with the silica alone. The extent of the interaction between the particles at the interface is not substantially impacted by the presence of surfactant at the interface. However, at the same time, the improvement of G' in the presence of the surfactant highlights that the number of interaction points between the particles is enhanced thanks to the surfactant molecules. This can be due to the surfactant adsorbed onto the silica and/or the surfactant molecules intercalated between the particles at the oil/water interface.

4 Conclusions

In this paper, we have explored the sensitivity and the limits of interfacial shear rheology in the presence of nanoparticles, surfactants, and mixture of particles and surfactants at the liquid/liquid interface. The majority of the experiments have been conducted with hydrophobic silica at the dodecane/water interface. The silica content was varied between 0.01 wt.% and 10 wt.%. The clean dodecane/water interface exhibits a liquid behavior while the presence of 10 wt.% of silica leads to a significant rigidification of the interface. The intermediate silica contents (0.01 wt.% – 1 wt.%) give access to viscoelastic interfaces. Three modes of mechanical solicitations, such as flow, creep and oscillatory, were addressed.

The results highlight that the technique of interfacial shear rheology based on DWR is sensitive to variations of the silica concentration and also to presence of surfactant in the silica adsorbed layer. On the one hand, the time after which the oily and aqueous phase are put into contact has to be taken into account. The measurements have to be performed only when the particles have reached a stationary state of adsorption. The time to reach this steady state depends on the silica concentration in the oil phase and can vary from 1 h up to 26 h. On the other hand, the sensitivity of the interfacial rheological methods is significantly impacted by the strength and the mode of the solicitation applied to the dodecane/water interface. It is recommended to use methods for which the shearing of the interface as well as the cumulated strain remain moderate. For flow and viscosity measurements, the method is not sufficiently sensitive to discriminate between the interfacial rheological behavior of the interfaces with 0, 0.1 and 1 wt.% of silica. The cumulated strain is too large to obtain reliable data. The continuous rotation of the ring in the same direction reduces the sensitivity and produces a lubricated friction of the ring on the silica film at the interface. Reducing the cumulated strain, with creep experiments, improves the sensitivity of the data. However, no difference between the systems with 0.01, 0.1 and 1 wt.% of silica were recorded. The oscillatory mode at low amplitude appears as the most sensitive method to conduct interfacial rheology experiments. It becomes possible to discriminate between the interfacial behavior of all the tested silica concentrations. In the presence of silica, the interface becomes viscoelastic. The interfacial elastic modulus G' increases regularly with the silica content. The resulting cumulated strain is much smaller than for the other tests while the ring oscillates around an equilibrium position. Consequently, the structure of the silica at the dodecane/water interface is not broken by the mechanical stress. With this mode, the ring gently deforms and produces only a soft solicitation of the adsorbed particles at the interface. The high sensitivity of the oscillatory mode based on amplitude sweep is confirmed by comparing the results obtained with surfactants, particles and mixture of surfactants and particles.

Supplementary Information The online version contains supplementary material available at https://doi.org/10.1007/s12633-022-02138-z.

Acknowledgements The authors thank David Israel (TA Instruments) and Pr. Lazhar Benyahia (Institut des Molécules et Matériaux du Mans, Le Mans Université) for their support and useful discussions on this work.

Author Contribution Thibault Roques-Carmes (TRC) and Philippe Marchal (PM) developed the methodology and conceptualization. Yuqing Wang (YW), Maud Lebrun (ML) and Diego Ramos (DR) conducted the majority of the experiments. TRC, PM, and VS analyzed the data. TRC and Véronique Sadtler (VS) participated to the project administration. TRC wrote the paper. All authors have read and agreed to the published version of the manuscript.

Funding This research received no specific grant from any funding agency in the public, commercial, or not-for-profit sectors.

Data Availability The data that support the findings of this study are available on request from the corresponding author, [TRC].

Declarations

Ethics Approval and Consent to Participate Not applicable for that section.

Consent for Publication Informed consent was obtained from all subjects involved in the study.

Competing Interests Not applicable for that section.

References

1. Mu L, Sprando RL (2010) Application of nanotechnology in cosmetics. Pharm Res 27:1746–1749
2. Mihranyan A, Ferraz N, Stromme M (2012) Current status and future prospects of nanotechnology in cosmetics. Prog Mater Sci 57:875–910
3. He X, Deng H, Hwang H-M (2019) The current application of nanotechnology in food agriculture. J Food Drug Anal 27:1–21
4. Kralova I, Sjoblom J (2009) Surfactants used in food industry: A review. J Dispers Sci Technol 30:1363–1383
5. Fernandez-Pena L, Guzman E (2020) Physicochemical aspects of the performance of hair conditioning formulations. Cosmetics 7:26
6. Chevalier Y, Bolzinger MA (2013) Emulsions stabilized with solid nanoparticles: Pickering emulsions. Colloids Surf A 439:23–34
7. Schmitt V, Destribats M, Backov R (2014) Colloidal particles as liquid dispersion stabilizer: Pickering emulsions and materials thereof. C R Physique 15:761–774
8. Yang Y, Fang Z, Chen X, Zhang W, Xie Y, Chen Y, Liu Z, Yuan W (2017) An overview of Pickering emulsions: Solid-particle materials, classification, morphology, and applications. Front Pharmacol 8:287
9. Wu J, Ma G-H (2016) Recent studies of Pickering emulsions: Particles make the difference. Small 12:4633–4648
10. Albert C, Beladjine M, Tsapis N, Fattal E, Agnely F, Huang N (2018) Pickering emulsions: Preparation processes, key parameters governing their properties and potential for pharmaceutical applications. J Control Release 309:302–332
11. Velandia SF, Marchal P, Lemaitre C, Sadtler V, Roques-Carmes T (2021) Evaluation of the repartition of the particles in Pickering emulsions in relation with their rheological properties. J Colloid Interface Sci 589:286–297
12. Uhlemann J, Costa R, Charpentier JC (2019) Product design and engineering in chemical engineering: Past, present state and future. Chem Eng Technol 42:1–18
13. Gani R, Bałdygab J, Biscans B, Brunazzi E, Charpentier JC, Drioli E, Feise H, Furlong A, Van Geem KM, de Hemptinne JC, ten Kate AJB, Kontogeorgis GM, Manenti F, Marin GB, Mansouri SS, Piccione PM, Povoa A, Rodrigo MA, Sarup B, Sorensen E, Udugama IA, Woodley JM (2020) A multi-layered view of chemical and biochemical engineering. Chem Eng Res Des 155:133–145
14. Roques-Carmes T, Aldeek F, Balan L, Corbel S, Schneider R (2011) Aqueous dispersions of core/shell CdSe/CdS quantum dots as nanofluids for electrowetting. Colloids Surf A 377:269–277
15. Mendoza AJ, Guzman E, Martinez-Pedrero F, Ritacco H, Rubio RG, Ortega F, Starov VM, Miller R (2014) Particle laden fluid interfaces: Dynamics and interfacial rheology. Adv Colloid Interface Sci 206:303–319
16. Deshmukh OS, van den Ende D, Cohen Stuart M, Mugele F, Duits MHC (2015) Hard and soft colloids at fluid interfaces: Adsorption, interactions, assembly & rheology. Adv Colloid Interface Sci 222:215–227
17. Velandia SF, Ramos D, Lebrun M, Marchal P, Lemaitre C, Sadtler V, Roques-Carmes T (2021) Exploring the link between interfacial and bulk viscoelasticity in reverse Pickering emulsions. Colloids Surf A 624:126785
18. Ramos D, Sadtler V, Marchal P, Lemaitre C, Benyahia L, Roques-Carmes T (2021) Insight into the emulsification process effect on particles distribution in Pickering emulsions: a series of rheological and gravimetric tests. Chem Eng Trans 86:1291–1296
19. Kovtun AI, Kartashynska ES, Vollhardt D (2021) Adsorption and viscoelastic properties of chitosan lactate at the liquid-gas interface. JCIS Open 1:100001
20. Jaensson N, Vermant J (2018) Tensiometry and rheology of complex interfaces. Curr Opin Colloid Interface Sci 37:136–150
21. Sagis LMC, Fischer P (2014) Nonlinear rheology of complex fluid-fluid interfaces. Curr Opin Colloid Interface Sci 19:520–529
22. Marczak W, Rogalski M, Modarressi A, Rogalska E (2016) A model of compression isotherms for analyzing particle layers. Colloids Surf A 489:128–135
23. Pradilla D, Simon S, Sjoblom J, Samaniuk J, Skrzypiec M, Vermant J (2016) Sorption and interfacial rheology study of model asphaltene compounds. Langmuir 32:2900–2911
24. Gong Y, Zhang Z, He J (2017) Deformation and stability of core−shell microgels at oil/water interface. Ind Eng Chem Res 56:14793–14798
25. Jaber A, Roques-Carmes T, Marchal P, Hamieh T, Benyahia L (2022) Interfacial viscoelastic moduli in a weak gel. J Colloid Interface Sci 622:126–134
26. Kragel J, Derkatch SR (2010) Interfacial shear rheology. Curr Opin Colloid Interface Sci 15:246–255
27. Golemanov K, Tcholakova S, Denkov N, Pelan E, Stoyanov SD (2012) Surface shear rheology of saponin adsorption layers. Langmuir 28:12071–12084
28. Klein CO, Theodoratou A, Ruhs PA, Jonas U, Loppinet B, Wilhelm M, Fischer P, Vermant J, Vlassopoulos D (2019) Interfacial Fourier transform shear rheometry of complex fluid interfaces. Rheol Acta 58:29–45
29. Renggli D, Alicke A, Ewoldt RH, Vermant J (2020) Operating windows for oscillatory interfacial shear rheology. J Rheol 64:141–160
30. Kamkar M, Bazazi P, Kannan A, Suja VC, Hejazi SH, Fuller GG, Sundararaj U (2020) Polymeric-nanofluids stabilized emulsions: Interfacial versus bulk rheology. J Colloid Interface Sci 576:252–263
31. Franck A, Hodder P (2009) Measuring the rheological properties of ultrathin films at the water-air and water-oil interface by using a novel double ring (DWR) geometry. Annual Transactions of the Nordic Rheology Society 17
32. Reynaert S, Moldenaers P, Vermant J (2007) Interfacial rheology of stable and weakly aggregated two-dimensional suspensions. Phys Chem Chem Phys 9:6463–6475

33. Barman S, Christopher GF (2014) Simultaneous interfacial rheology and microstructure measurement of densely aggregated particle laden interfaces using a modified double wall ring interfacial rheometer. Langmuir 30:9752–9760
34. Jaishankar A, Sharma V, McKinley GH (2011) Interfacial viscoelasticity, yielding and creep ringing of globular protein-surfactant mixtures. Soft Matter 7:7623–7634
35. Thijssen JHJ, Vermant J (2018) Interfacial rheology of model particles at liquid interfaces and its relation to (bicontinuous) Pickering emulsions. J Phys Condens Matter 30:023002
36. Pinaud F, Geisel K, Massé P, Catargi B, Isa L, Richtering W, Ravaine V, Schmitt V (2014) Adsorption of microgels at an oil-water interface: correlation between packing and 2D elasticity. Soft Matter 10:6963–6974
37. Golemanov K, Tcholakova S, Denkov N, Pelan E, Stoyanov SD (2013) Remarkably high surface visco-elasticity of adsorption layers of triterpenoid saponins. Soft Matter 9:5738–5752
38. Maestro A, Santini E, Zabiegaj D, Llamas S, Ravera F, Liggieri L, Ortega F, Rubio RG, Guzman E (2015) Particle and particle-surfactant mixtures at fluid interfaces: Assembly, morphology, and rheological description. Adv Condens Matter Phys 917516:1–17
39. Rahman SE, Laal-Dehghani N, Barman S, Christopher GF (2019) Modifying interfacial interparticle forces to alter microstructure and viscoelasticity of densely packed laden interfaces. J Colloid Interface Sci 536:30–41
40. Sun Q, Liu W, Li S, Zhang N, Li Z (2021) Interfacial rheology of foam stabilized by nanoparticles and their retention in porous media. Energy Fuels 35:6541–6552